Molecular Biology of the Cell
Vol. 21, 1825–1835, June 1, 2010

Autophagic Cell Death in *Dictyostelium* Requires the Receptor Histidine Kinase DhkM

Corinne Giusti, Marie-Françoise Luciani, Sarina Ravens, Alexandre Gillet, and Pierre Golstein

Centre d'Immunologie de Marseille-Luminy, Faculté des Sciences de Luminy, Aix Marseille Université, Marseille F-13288, France; Institut National de la Santé et de la Recherche Médicale U631, Marseille F-13288, France; and Centre National de la Recherche Scientifique Unité Mixte de Recherche 6102, Marseille F-13288, France

Submitted November 23, 2009; Revised March 26, 2010; Accepted March 29, 2010
Monitoring Editor: Carole Parent

Dictyostelium **constitutes a genetically tractable model for the analysis of autophagic cell death (ACD). During ACD,** ***Dictyostelium*** **cells first transform into paddle cells and then become round, synthesize cellulose, vacuolize, and die. Through random insertional mutagenesis, we identified the receptor histidine kinase DhkM as being essential for ACD. Surprisingly, different DhkM mutants showed distinct nonvacuolizing ACD phenotypes. One class of mutants arrested ACD at the paddle cell stage, perhaps through a dominant-negative effect. Other mutants, however, progressed further in the ACD program. They underwent rounding and cellulose synthesis but stopped before vacuolization. Moreover, they underwent clonogenic but not morphological cell death. Exogenous 8-bromo-cAMP restored vacuolization and death. A role for a membrane receptor at a late stage of the ACD pathway is puzzling, raising questions as to which ligand it is a receptor for and which moieties it phosphorylates. Together, DhkM is the most downstream-known molecule required for this model ACD, and its distinct mutants genetically separate previously undissociated late cell death events.**

INTRODUCTION

The term autophagic cell death (ACD) now tends to designate cell death that not only shows signs of autophagy but also requires it (Berry and Baehrecke, 2008; Eisenberg-Lerner *et al*., 2009). Although the molecular mechanisms of autophagy itself have been thoroughly studied, those of subsequent cell death are essentially unknown. We have been investigating such mechanisms in the protist *Dictyostelium discoideum*, where ACD shows autophagy (de Chastellier and Ryter, 1977; Tresse *et al*., 2008), is dependent on the atg1 autophagy gene (unpublished data), and also requires an analyzable second signal as shown below.

Dictyostelium vegetative cells grow as single amoebae in rich medium, but when starved they start a developmental program leading to a fruiting body comprising a multicellular stalk. In this stalk, cells are dying or dead, thus providing an example of developmental cell death. The latter can be mimicked and studied in cell monolayers in vitro (Kay, 1987), where this model organism shows several advantages (Giusti *et al*., 2009b). Its small, compact, sequenced, and haploid genome facilitates insertional mutagenesis and other genetic approaches. Also, in *Dictyostelium* cells there is no apoptosis machinery that could interfere with, substitute for, or be triggered upon, autophagic cell death. Finally, and most importantly, induction of ACD in *Dictyostelium* in a monolayer requires two distinct signals. A first signal is starvation, which induces atg1-requiring autophagy. A second signal is differentiation-inducing factor-1 (DIF-1) (Kay, 1987; Morris *et al*., 1987), which is required for induction of cell death in vitro (Kay, 1987; Cornillon *et al*., 1994; Levraud *et al*., 2003). Under our experimental conditions, DIF-1 is not made in sufficient amounts by starving cells in vitro. The cells thus require addition of exogenous DIF-1 to proceed to ACD. Thus, in this model, starvation is sufficient to induce autophagy but not ACD. Induction of the latter requires autophagy plus a qualitatively distinct second signal, DIF-1.

Addition of DIF-1 to starved cells triggered a sequence of events leading to ACD (Cornillon *et al*., 1994; Levraud *et al*., 2003; Giusti *et al*., 2009b). This sequence included within 10–16 h the emergence of strikingly polarized paddle cells. Then, after IP3R- and Talin B-dependent events (Lam *et al*., 2008; Giusti *et al*., 2009b), two main transitions led to cell death. The first is a paddle-to-round cell transition, accompanied by F-actin depolymerization (Levraud *et al*., 2003). A few hours later, round cells began to vacuolize, undergoing a second transition from round cells to vacuolization. Membrane permeabilization and cell death ensued. No direct molecular information is available as to this second transition and cell death.

To investigate the molecular mechanism of DIF-1-induced ACD, taking advantage of the haploidy of the *Dictyostelium* genome, we have been using random mutagenesis (Kuspa and Loomis, 1992) followed by induction of ACD to select or screen for nonvacuolizing mutant cells (Giusti *et al*., 2009b). This led us to identify the receptor histidine kinase DhkM as a molecule required for the normal course of ACD. Distinct DhkM mutants showed different nonvacuolizing phenotypes, reflecting arrest at distinct stages of the ACD pathway. Insertion mutants initially obtained by random insertional mutagenesis acted like dominant negatives by in-

This article was published online ahead of print in *MBoC in Press* (http://www.molbiolcell.org/cgi/doi/10.1091/mbc.E09–11–0976) on April 7, 2010.

Address correspondence to: Pierre Golstein (golstein@ciml.univ-mrs.fr).

terrupting the paddle-to-round transition, stopping the course of ACD at the paddle cell stage, thus preventing in particular vacuolization and death. Deletion mutants obtained by targeted mutagenesis acted more downstream in the ACD pathway and prevented vacuolization and morphological cell death (checked by loss of integrity of the plasma cell membrane) but not clonogenic cell death (checked by loss of ability to multiply upon addition of HL5 rich medium). In addition, exogenous 8-bromo-cAMP overcame these arrests. Together, DhkM mutants furthered the genetic analysis of late ACD events, dissociating in particular vacuolization and morphological from clonogenic cell death.

MATERIALS AND METHODS

Cells, Cell Culture, Induction of Cell Death, and Microscopy

The parental *Dictyostelium* strains used in this report were HMX44A (for detailed derivation, see Levraud *et al*., 2003), DH1, and JH10. Cells were grown in HL5-modified medium (Cornillon *et al*., 1994) alone or supplemented with 10 μg/ml blasticidin (Invitrogen, Carlsbad, CA) for the transformants. The thymidine auxotroph JH10 cells were grown in HL5 supplemented with 100 μg/ml thymidine (Sigma-Aldrich, St. Louis, MO). For autophagic cell death induction (Cornillon *et al*., 1994; Levraud *et al*., 2003), exponentially growing vegetative cells were washed once in phosphate-buffered saline (Soerensen buffer [SB]) and incubated in SB containing 3 mM cAMP (Sigma-Aldrich) for 8 h at 22°C in Lab-Tek culture chambers (155380; Nalge Nunc International, Rochester, NY) at a concentration of 3×10^5 cells/ml/chamber. Cells were then washed in SB and incubated at 22°C in either SB alone or SB containing the differentiation factor DIF-1 (DN1000; Affiniti Research Products, Exeter, United Kingdom) at a final concentration of 10^{-7} M. After the indicated period, cells in the Lab-Tek chambers were examined using an Axiovert 200 microscope (phase contrast, oil immersion, 100×; Carl Zeiss, Jena, Germany) and photographed using an Axiocam MRC camera controlled by AxioVision 4.7 (Carl Zeiss). Images were subsequently treated with Photoshop (Adobe Systems, Mountain View, CA) or Graphic Converter. Figures were assembled using Illustrator (Adobe Systems).

For cellulose staining, cells in the Lab-Tek chambers were treated with calcofluor white M2R (stock solution at 1% in water; F3543, Sigma-Aldrich) at a final concentration of 0.01% and observed after 10 min by fluorescence microscopy. For experiments on wrapping cells, cells adhering to cellulose shells could been seen readily in HMX44A.DhkM^{del} cells 20–40 h after addition of DIF-1, thus with endogenous cells. Alternatively, fresh vegetative cells were added to DIF-1–treated cells. Specifically, HMX44A, HMX44A.DhkM^{del}, DH1, or DH1.DhkM^{ins} cells were starved and treated with DIF-1 as indicated above. Usually, 40 h after addition of DIF-1, fresh vegetative cells (usually HMX44A.DhkM^{del} or other strains with similar results) were added (10^5cell/100μl/chamber). After 2 h at 22°C, cells were observed by phase contrast microscopy.

For phalloidin staining to detect F-actin, to each 1 ml of SB-containing chamber 0.3 ml of 4% paraformaldehyde in SB was carefully added; after 10 min at 22°C, cells were washed in SB and 1 ml of SB was added containing 10 μl of a stock solution of Alexa Fluor 488-phalloidin (A-12379; Invitrogen; 300 U in 1.5 ml of methanol); this was followed with overnight incubation. To detect acidic vacuoles, we used the acidotropic dye LysoSensor Blue DND-167 (LB; L7533, Invitrogen), which seems to accumulate in acidic organelles as the result of protonation. Cells in Lab-Tek chambers were labeled at the indicated times with 5 μM LB for 10 min and then examined by confocal microscopy (LSM 510, META UV; Carl Zeiss) with a 63× oil immersion objective, with the scanning module at 1024×1024 pixel resolution, 8 bits, using a scan average of 4 with a 405 nm excitation laser and a band pass of 420–480.

For viability tests, fluorescein diacetate (FDA; F7378, Sigma-Aldrich; stock solution at 10 mg/ml in acetone) was used at a final concentration of 50 μg/ml for 10 min. In cell regrowth assays (Levraud *et al*., 2003), HMX44A wild-type or mutant cells were incubated in Lab-Tek chambers as described above, either without or with 10^{-7} M DIF-1. After a variable period at 22°C, to initiate regrowth 0.5 ml of SB was removed from and 1 ml of HL-5 was added to each Lab-Tek chamber. After 48–72 h of additional incubation at 22°C, vegetative cells resulting from regrowth were counted in an hemocytometer. For each time point of incubation in SB, the percentage of surviving cells in the presence of DIF-1 was deduced from the ratio of cells regrown after incubation with DIF-1 to that of cells regrown after incubation in the absence of DIF-1.

To assess the developmental ability of wild-type or DhkM mutant DH1 and JH10 cells, exponentially growing cells were harvested from flasks, washed twice with SB, and resuspended by pipetting in SB. Fifty milliliters of SB containing 2×10^6 cells was spotted on Petri dishes coated with a 2% agar layer containing thymidine 100 μg/ml when JH10 cells were tested. On incubation at 23°C, wild-type fruiting bodies were obtained after ~24 h. Wild-type and mutant development products were photographed at ~40 h by using a stereomicroscope.

Each experiment shown in this report was performed at least three times with similar results, unless mentioned otherwise.

Random Insertional Mutagenesis and Screening

For each transfection, 2×10^7 exponentially growing vegetative cells were electroporated with 15 μg of BamHI-linearized pUCBsrΔBamHI vector in 800 μl of ice-cold electroporation buffer (10 mM Na_2HPO_4, KH_2PO_4, pH 6.1, and 50 mM sucrose) in the presence of 4 U of the DpnII restriction enzyme (catalog no. 1992; New England Biolabs, Ipswich, MA) using a Gene Pulser (1 kV; 3 μF; expected pulse time: 0.6–1.1 ms; Bio-Rad Laboratories, Hercules, CA). Cells were incubated in HL5 medium at 22°C for 24–48 h and then 10 μg/ml blasticidin was added to select transformants during a further period of culture of 5–10 d. After selection, 12×10^6 transformants were subjected to cell death induction in monolayer in 75-cm^2 flasks (Falcon; BD Biosciences Discovery Labware, Bedford, MA) as described above (upscaled to 20 ml final volume). After 48 h, DIF-containing SB was removed and replaced with HL5 medium to enable growth of surviving cells. When enough cells had been obtained, a second similar round of cell death induction and selection was performed. Surviving cells were grown for 6 d, and a suspension of 10^6 cells/ml HL5 was used to distribute by cell sorting (BD-FACS Vantage, BD Biosciences, Franklin Lakes, NJ) one cell per HL5-containing flat-bottomed well of 96-well plates. Cells were left to grow at 22°C until near confluence and then subjected in wells to DIF-1–induced cell death. After 24–48 h, screening by phase contrast microscopy (Axiovert 200, 32×; Carl Zeiss) was conducted to look for wells with cells showing no vacuolization, thus putatively derived from mutant cells. Cells in these wells were allowed to regrow by addition of HL5, and resistance to death was verified by tests in Lab-Tek chambers as described above.

Identification of the Mutated Gene by Inverse Polymerase Chain Reaction (PCR)

The gene mutated in CG5 mutant cells was identified by inverse PCR (Keim *et al*., 2004). In brief, 20 μg of the CG5 genomic DNA (gDNA) was digested by the restriction enzyme AluI that cuts frequently in the *Dictyostelium* genome. Purified cut gDNA was ligase (New England Biolabs)-circularized in a final volume of 400 μl. Circular DNA was purified and resuspended in 50 μl of H_2O. One microliter was amplified by PCR using pUCBsrΔBamHI primers (5′-GAA TTG CCG CTC CCA CAT GA-3′ and 5′-GCG ATT GGT AGT GCA GTT TC-3′) (2 min at 95°C; then 35 cycles of 30 s at 95°C, 30 s at 58°C, 4 min at 68°C; and then 10 min at 68°C). The PCR product was sequenced and the gene corresponding to the vector flanking regions was identified by homology search within the *Dictyostelium* genome.

Targeted Mutagenesis

To obtain a deletion mutant in DhkM (3083 base pairs deleted), we prepared a homologous recombination construct bearing 5′(from nucleotide [nt] 859 to nt 1511) and 3′ arms (from nt 4592 to nt 5036) made separately by PCR from gDNA. The 5′ and 3′ arms were ligated by PCR then introduced into pGEM-T Easy (Promega, Madison, WI). After plasmid linearization with BamHI, a blasticidin resistance (bsR) cassette was inserted between the arms. This construct was verified by digestions and sequencing. The plasmid was digested with SwaI and HhaI, and then the fragment containing arms and bsR was purified from the agarose gel and transfected in HMX44A, JH10, or DHI strains by electroporation (1 kV; 3 μF using a Gene Pulser). Cells were selected for resistance to 10 μg/ml blasticidin and cloned by limiting dilution. Homologous recombination was verified by PCR and Southern blots. For DhkM insertional mutagenesis, the 5′ arm was from nt 5472 to nt 6114 and the 3′ arm from nt 6122 to nt 6568. Before electroporation, the arms flanking the bsR cassette were extracted from the pGEM vector by digestion with BseRI and HincII restriction enzymes.

Expression Tested by Reverse Transcription (RT)-PCR

Preparations of 0.5 μg of total TRIzol-extracted RNA from HMX44A wild type (wt), DhkM^{ins}, or DhkM^{del} cells were reverse transcribed using the QuantiTec Reverse Transcription kit (QIAGEN, Valencia, CA) according to the manufacturer's instructions. One microliter of each reaction was used for PCR, using the primers required to amplify the following products (Figure 1C): alpha, 5′GGAGGTGGAAATAATAAAAATAATGGTGGTG3′ and 5′GTTTGGATCCGGTGGTGGTAGTTGAGGTGG3′; beta, 5′GTTTCCATGGGGTGGTGATGATAGCGCTC3′ and 5′GTTTAAGCTTCATAATCTGGTATTGAAGTTGACG3′; gamma, 5′GTTTGGATCCCGAACTGGTATTCCAATACCAAAATCTG3′ and 5′GTTTAAGCTTCATAATCTGGTATTGAAGTTGACG3′; and delta, 5′CCAGTACAATTTCAAGCACCATTGGC3′ and 5′TGGTTGTTGTTTTAAAACACCTAAATTACTTGAGAGGG3′.

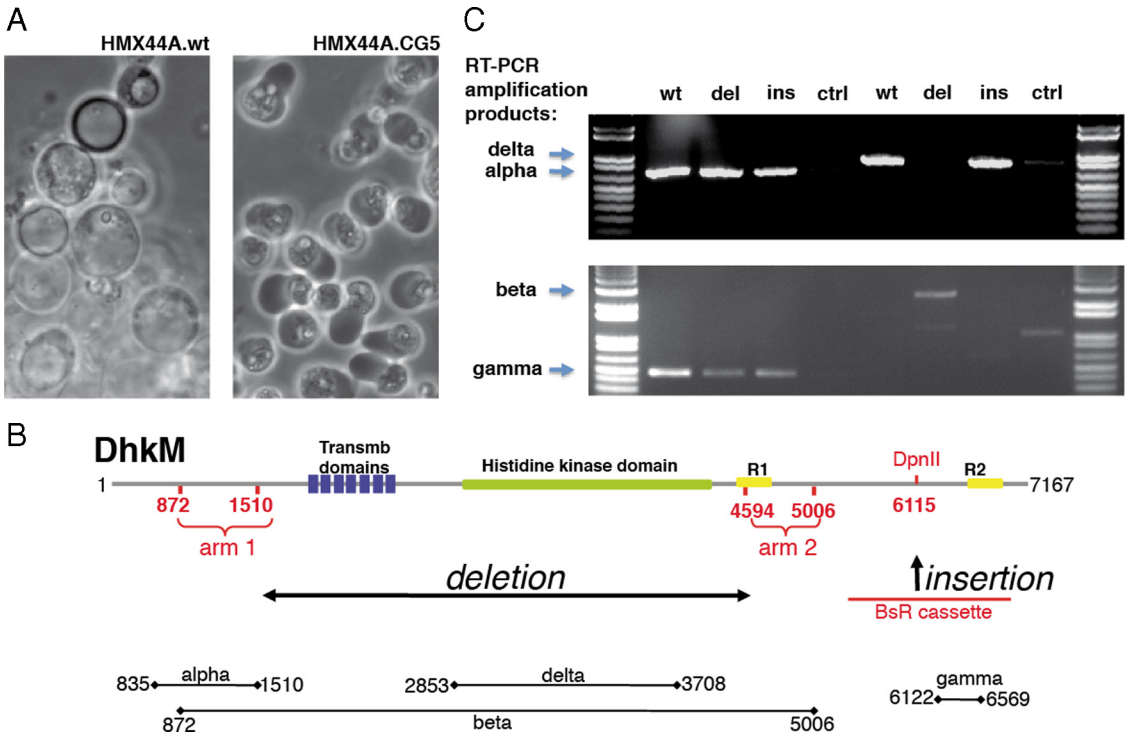

Figure 1. The CG5 cell death mutant and its mutated DhkM gene. (A) Forty hours after induction of autophagic cell death by addition of DIF-1 to starved cells, wild-type HMX44A *Dictyostelium* cells vacuolized (left), whereas mutant HMX44A.CG5 cells did not (right). This was shown in four of four experiments. (B) Top, DhkM gene and putative protein. The gene mutated in CG5 cells was identified by plasmid rescue as DhkM. The DhkM genomic sequence includes a short intron (nt 2038–2111). The numbers refer to the 7167-nt coding sequence (however, Dictybase indicates a 2388-amino acid protein, which would correspond to a 7164-nt coding sequence). Names above the line refer to domains of the corresponding putative protein, including from left to right an extracellular region, seven transmembrane domains, the histidine kinase domain, and two putative response regulator receiver regions (R1 and R2) (http://dictybase.org/db/cgi-bin/dictyBase/polypeptide/domains.pl?protein_id=DDB0220020.P). Experimental alterations to the gene are shown in red. Middle, sites of deletion and insertion by targeted mutagenesis. To the right, the insertion of the blasticidin resistance cassette in the DpnII site at residue 6115 was between the putative response regulator receiving regions as for the initial insertion by random mutagenesis. More to the left, arms 1 and 2 were used for targeted mutagenesis, leading to a deletion of in particular the transmembrane and the histidine kinase domains, replaced by the blasticidin resistance cassette. Bottom, amplification products obtained using the pairs of primers described in *Materials and Methods*, in the RT-PCR reactions analyzed in C. (C) RT-PCR products testing the expression of wild-type and DhkM mutants mRNA. RNAs from wild-type (wt), DhkM^{del} (del), and DhkM^{ins} (ins) mutant HMX44A cells were extracted at 16 h post-DIF-1. After reverse transcription, PCR reactions were prepared using primers amplifying the alpha, delta, gamma, and beta fragments as defined in B, bottom. Control groups (ctrl) included no reverse transcriptase. Markers were the 1kb plus DNA ladder (Invitrogen).

Functional Restoration with 8-Bromo-cAMP

HMX44A or JH10 cells were incubated in Lab-Tek culture chambers and autophagic cell death was induced as described previously. At the indicated time after addition of DIF-1, 8-bromo-cAMP (B7880; Sigma-Aldrich), or sorbitol (S3889; Sigma-Aldrich) or cAMP as controls, were added at a final concentration of 20 mM. The regrowth tests with HMX44A.DhkM^{ins} cells were otherwise performed as described above. The regrowth ability of DhkM^{ins} cells in the absence of DIF-1 and 8-bromo-cAMP was defined as 100%.

RESULTS

Isolation of Mutant Cells with Impaired Autophagic Cell Death and Identification of the Mutated Gene as DhkM

After mutagenesis through random insertion of a plasmid containing a blasticidin-resistance cassette, 1.2×10^7 HMX44A cells were selected for blasticidin resistance, enriched for cell death-resistant mutants, cloned in microplate wells, induced to die through starvation and addition of DIF-1, and screened for absence of marked vacuolization. Of ~1350 screened clones, 21 scored positive. We chose to proceed with one of these 21 clones, named CG5. When retested in Lab-Tek chambers, wild-type cells showed the usual pattern of vacuolization 40 h after addition of DIF-1, but CG5 mutant cells were arrested at the paddle cell stage and showed no vacuolization (Figure 1A). This mutant is the same as the X mutant mentioned in a previous review (Giusti *et al*., 2009b).

By Southern blots, only one insertion of the blasticidin-resistance cassette of the inactivating plasmid was detected in the CG5 genome (data not shown). The gene it disrupted was identified by plasmid rescue as encoding the receptor histidine kinase DhkM. This DhkM gene putatively encodes an extracellular region, a seven-transmembrane domain, a histidine kinase domain, and two putative response regulator receiver regions (Goldberg *et al*., 2006; Figure 1B). In the CG5 mutant, the inactivating plasmid had inserted in the DpnII site at nt 6115 of the DhkM coding sequence (Figure 1B).

We prepared by targeted mutagenesis two types of mutants of the DhkM gene. In insertion mutants (*ins*), the blasticidin resistance cassette was inserted at the site of insertion of the initial CG5 mutant in the 3′ region of DhkM between the putative response regulator receiving regions (Figure 1B). These *ins* mutants may not affect membrane expression of the proteins but may affect signal transduction. Deletion mutants (*del*) were obtained using a construct where the blasticidin

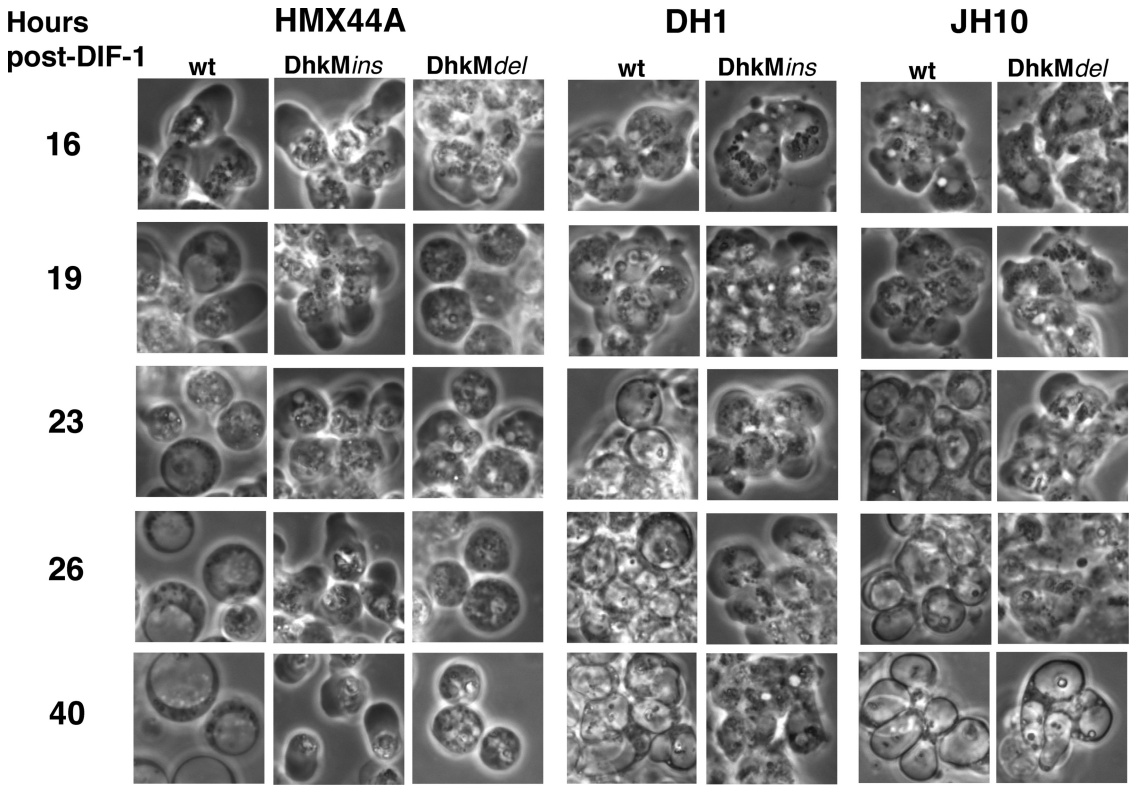

Figure 2. Time course of autophagic cell death in wild-type and DhkM mutant cells. Cells from *Dictyostelium* strains (HMX44A, DH1, and JH10), either wild type or bearing a DhkM insertion or deletion mutation, have been tested in parallel and are shown as a function of time after addition of DIF-1. DhkM mutations markedly delayed or suppressed vacuolization, however less so in JH10 cells. When tested in the same HMX44A background, nonvacuolizing DhkM *ins* or *del* mutant cells looked markedly different, enriched in either paddle or round cells, respectively. The same scale has been used throughout. Such a complete experiment was done three times, and partial experiments many more times, with similar results.

resistance casette was flanked with arm 1 and arm 2 (Figure 1B), the insertion of which led to the replacement of most of the DhkM genomic DNA including that encoding the transmembrane and histidine kinase domains. In these *del* mutants, what may be left of the DhkM protein should be functionally severely impaired. Insertions and deletions were verified by PCR and Southern blots (data not shown). DhkM *ins* (designated DhkM^{ins}) and *del* mutants (designated DhkM^{del}) were prepared in three *Dictyostelium* strains (HMX44A, JH10, and DH1), because these strains can differ in phenotypic expression of given mutations (Lam *et al*., 2008; Giusti *et al*., 2009b). Also, a DhkM mutant was prepared in atg1-mutant cells to test a possible effect of DhkM on necrotic cell death (Kosta *et al*., 2004). Together, six independent DhkM mutants were obtained and tested: CG5, HMX44A.DhkM^{ins}, HMX44A.DhkM^{del}, HMX44A.atg1-3.DhkM^{ins}, DH1.DhkM^{ins}, and JH10.DhkM^{del}.

We investigated the mRNA expression of HMX44A wild-type and DhkM mutants by RT-PCR. Primers (see *Materials and Methods*) were chosen to give the alpha, beta, gamma, and delta amplification products depicted in Figure 1B. These primers were first tested by PCR on genomic DNA from wild-type HMX44A cells, yielding no amplification when each primer was tested in isolation, and only one band of amplification, at the expected size, for each of the selected pairs of primers (data not shown). When tested in RT-PCR (Figure 1C), each of the alpha and gamma pairs gave a band at all tested times (including for vegetative cells), but not in the absence of reverse transcriptase, by using RNA prepared from wild-type but also from DhkM^{ins} and DhkM^{del} mutant cells. As expected, the delta amplification product could be detected in wild-type and DhkM^{ins}, but not in DhkM^{del}, extracts, and the beta amplification product showed the reciprocal pattern. Thus, in the *ins* mutant the mRNA still existed and read through the insertion, at least until nt 6569 of wt DhkM. The insert was ~1.6 kb; the total length of the mRNA may thus be at least 8.2 kb. Similarly, the total length of the *del* mRNA may be at least 5.1 kb. Together, these results showed that expression of wild-type and mutant DhkM mRNA was constitutive. Also, part of the DhkM message was present in both the insertion and the deletion DhkM mutants.

DhkM Insertion and Deletion Mutations Markedly Delayed Vacuolization, but Inhibited Distinct Stages of the ACD Pathway

We chose HMX44A as our standard strain to investigate in more detail the DhkM mutant ACD phenotype(s). Both HMX44A wild-type and DhkM mutant cells showed emergence of paddle cells 10–16 h after addition of DIF-1 (Levraud *et al*., 2003; data not shown). After the paddle cell stage and a brief round cell stage, most wild-type cells vacuolized (Levraud *et al*., 2003; Figure 2, column 1 from the left). In marked contrast, neither DhkM mutants vacuolized within the indicated time span, and only much later (after 60 h) did a sizable proportion of vacuolar cells appear. Although both DhkM *ins* and *del* mutants showed no vacuolization, unexpectedly they differed with regard to their ACD phenotypes. HMX44A.DhkM^{ins} showed persistence of paddle cells (Figure 2, column 2), indicating impairment of

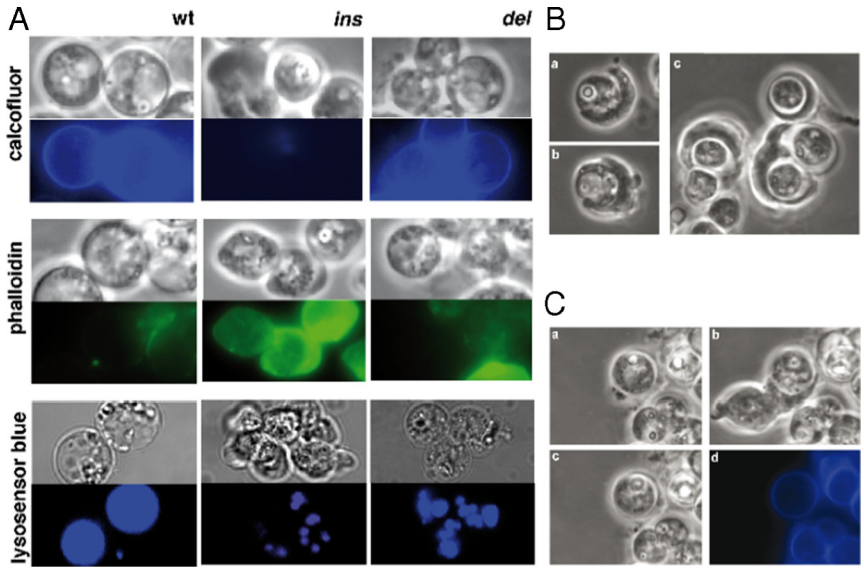

Figure 3. Localization of the DhkM *ins* and *del* mutants in the ACD pathway. (A) HMX44A wt or DhkM *ins* or *del* mutant cells were subjected to starvation and DIF-1 and then tested at 40 h post-DIF-1 either with calcofluor (top row), showing that cellulose synthesis occurred in *del* not in *ins* mutants; with phalloidin (middle row), showing that actin was polymerized in *ins* but not *del* mutants; or with LysoSensor Blue (lower row), showing that small acidic vacuoles persisted in both mutants; the vacuoles seemed larger here in *del* than in *ins* cells, but they were often quite similar in size. All experiments in this figure have been done using phase contrast and fluorescence, except that with LysoSensor Blue, which used differential interference contrast and confocal microscopy. Experiments testing each reagent have been performed separately, each at least three times with similar results. (B) Cells wrapping cellulose shells among HMX44A.DhkM^{del} cells (a and b) 40 h after addition of DIF-1 with no added fresh cells and 2 h after addition of fresh vegetative cells to 40 h-DIF-1–induced HMX44A.DhkM^{del} cells (c). (C) Fresh vegetative cells were added to 40 h-DIF-1–induced HMX44A.DhkM^{del} cells. (a–c) An added fresh "wrapping" cell was dislodged, but round cells were not, upon pipetting 1 ml of buffer 10 times using 1-ml tips. (d) Cells were then labeled with calcofluor, showing that the round cells were encased in a cellulose shell probably contributing to their adherence to the substrate and to the wrapping by fresh cells.

the paddle-to-round transition. This also was observed in the initial CG5 random insertion mutant (Figure 1A), whose phenotype was therefore accounted for by the DhkM targeted *ins* mutation. In marked contrast, HMX44A.DhkM^{del} cells showed persistence of postpaddle round cells (Figure 2, column 3), indicating impairment of the round-to-vacuolar transition. The complete experiment shown in Figure 2 was done three times with similar results, which also were obtained in each of >15 experiments comparing the DIF-1–induced cellular phenotypes in HMX44A.DhkM^{ins} ("paddles") and HMX44A.DhkM^{del} ("round") mutant cells. In one of these experiments, these observations were quantified at 24 h post-DIF-1 by counting for each group 200 identifiable cells outside or lining clumps. Percentages for HMX44A wild-type cells were 15% paddle cells, 16% round cells, and 39% vacuolated cells (30% were vegetative-like); for DhkM^{ins} cells, 95% paddle cells and neither round nor vacuolated cells (5% were vegetative-like); and for DhkM^{del} cells, 22% paddle cells, 76% round cells, and 2% vacuolated cells. Although all the experiments shown in this report used 100 nM DIF-1, similar results were obtained with a range of 50–400 nM DIF-1 (data not shown). Together, on the HMX44A background, two independently obtained *ins* mutants (CG5 and HMX44A.DhkM^{ins}) showed persistence of paddle cells, whereas a *del* mutant passed the paddle cell stage and showed persistence of round cells. These distinct *ins* or *del* nonvacuolar phenotypes corresponded, respectively, to the consecutive paddle cell and round cell stages of ACD in wild-type cells, indicating that *ins* inhibited the ACD pathway upstream of *del* (see below). Together, HMX44A.DhkM *ins* and *del* mutants all showed no or only very late vacuolization, but they differed as to which prevacuolization stage they blocked.

We then checked the impact of DhkM mutations on *Dictyostelium* strains other than HMX44A (which derives from the initial V12M2 Raper strain). Cells from the DH1 and JH10 strains (both deriving from the distinct NC-4 Raper strain; Raper, 1935) were subjected to DhkM-targeted mutagenesis. Both DH1.DhkM^{ins} and JH10.DhkM^{del} mutant cells showed delay in vacuolization, resulting in less vacuolar cells at given early times after DIF-1. However, this effect was less clear-cut than in HMX44A.DhkM mutants and more marked on DH1 than on JH10 cells (Figure 2, compare columns 4 and 5 and columns 6 and 7) in which the types of mutation (*del* vs. *ins*) also differed. Quantification was more difficult than for HMX44A cells, because most cells were in clumps and paddle and round cells could often not be distinguished with certainty. We therefore counted cell clumps containing no visible vacuolated cells or containing at least one or often many more vacuolated cells. In one experiment for DH1 cells at 24 h post-DIF-1, of 100 wild-type cell clumps 92 contained vacuolated cells, whereas of 100 DhkM^{ins} cell clumps, none contained vacuolated cells. For JH10 cells at 23 h post-DIF-1, of 100 wild-type cell clumps 97 contained vacuolated cells, whereas of 100 DhkM^{del} cell clumps only two contained vacuolated cells. Together, a delay in vacuolization was observed in each of five independent DhkM single mutants, obtained in three distinct backgrounds.

DhkM Insertion Mutations Inhibited the ACD Pathway Upstream and Deletion Mutations Downstream of Actin Depolymerization and Cellulose Shell Synthesis

As indicated above, DhkM *ins* and *del* mutations apparently inhibited distinct stages of ACD. We tried to localize more precisely the site(s) of impact of the DhkM mutations, by mapping their effects with regard to other known traits of ACD. Forty hours after DIF-1 addition to HMX44A cells, calcofluor stained blue many *del* or wt cells but stained blue only a few *ins* cells (Figure 3A, top row), showing that cellulose synthesis was delayed in these cells. DhkM^{del} mutant cells synthesized a cellulose shell for longer than wild-type cells, because they died much later (see below). This led to surviving round *del* cells surrounded by cellulose shells adhering to the plastic substrate. Rare mobile cells which persisted 40 h after addition of DIF-1 tended to wrap these cellulose shells (Figure 3B, a and b) at a frequency of 3 ± 2% of individualized round cells. To allow easier study of this unexpected observation, we increased this frequency by adding vegetative cells to 40 h-DIF-1–induced *del* cells. Two hours after this addition, the frequency of wrapped cells

(Figure 3Bc) was 29 ± 7% of individualized round cells. This frequency of approximately one third stayed constant for at least 5 h (data not shown). By videomicroscopy, the round cells displayed intracellular movements but seemed immobile relative to the substrate (Supplemental Videos 1 and 2), and strong pipetting dislodged wrapping cells but not round cells (Figure 3C, a–c), showing that round cells adhered to the substrate, probably through their cellulose shell (Figure 3Cd). Wrapping cells showed revolving movements (in either direction; data not shown) similar to those of an eccentric wheel, followed by their departure and eventually rewrapping of the same round cell by another fresh cell (Supplemental Videos 1 and 2). These events required no obvious self- or nonself-preference between the cells at play, and the round cells could be alive or dead (data not shown). These observations are probably due to the presence of plastic-stuck cellulose shells, acting as pegs around which fresh cells wrapped themselves and turned. Indeed, *Dictyostelium* cells can express proteins with cellulose-binding domains (Wang *et al*., 2001; also see http://dictybase.org/, cellulose-binding).

F-Actin–staining phalloidin stained green most *ins* but only a few wt or *del* mutant cells (Figure 3A, middle). Thus, cellulose synthesis and F-actin depolymerization had not occurred in most *ins* cells but had occurred in most *del* cells, showing that both F-actin depolymerization (leading to cell rounding; Levraud *et al*., 2003) and cellulose synthesis were initiated downstream of *ins* but upstream of *del*, contributing to map *ins* upstream of *del*.

The DhkM^{del} mutation prevented vacuolization, namely, the emergence of the huge acidic vacuole that ends up occupying most of the cell volume. In yeast, a similarly huge vacuole seems to be made by fusion of smaller vacuoles (Dove *et al*., 2009). We wondered whether acidic vacuoles of significant size could already be detected in the round cells accumulating in the *del* mutants. Indeed, LysoSensor Blue staining identified in each DIF-1–induced wild-type cell the usual huge vacuole, and in each DhkM mutant cell several smaller vacuoles (Figure 3A, bottom row). These observations were in line with the possibility that the fusion of these small vacuoles was important for the emergence of the large vacuole and might be prevented in the *del* mutants.

Thus, all DhkM mutants on the HMX44A background impaired the DIF-1–induced ACD pathway. However, by the time wild-type cells had vacuolized, the *ins* mutant cells had kept paddle cell morphology and F-actin and had not acquired a cellulose shell and thus had not undergone the paddle-to-round transition. In contrast, the *del* mutant cells had become round, lost F-actin, and synthesized a cellulose shell but had not vacuolized; thus, they had not undergone the subsequent round-to-vacuolar transition. This showed that the ACD pathway was inhibited by DhkM mutants at two distinct stages, by *ins* at the paddle-to-round transition and by *del* at the round-to-vacuole transition. Thus, the order of functional involvement, as shown by the corresponding mutations, was (induction by DIF-1) - iplA, talin B, DhkM^{ins} - (F-actin depolymerization, cellulose synthesis) - DhkM^{del} - (vacuolization) (see Figure 6).

DhkM Insertion Mutants Prevented Morphological and Clonogenic Cell Death; DhkM Deletion Mutants Prevented Morphological but Not Clonogenic Cell Death

We wondered whether impaired vacuolization in DhkM mutant cells was accompanied by impaired cell death. This was assessed in strain HMX44A cells by regrowth tests (checking clonogenic cell death) and by FDA and propidium iodide (PI) staining (checking morphological cell death). In regrowth tests, numbers of cells regrown in experimental groups initially subjected to DIF-1 were expressed as percentages of numbers of cells regrown in groups not subjected to DIF-1. When HL5 rich medium was added at 24 h post-DIF-1, as anticipated for wild-type cells, the regrowth with DIF-1 was only 40% of the regrowth without DIF-1, reflecting irreversible DIF-1–induced clonogenic cell death (Figure 4A, 24 h, left column). At 24 h, the DhkM^{ins} mutant cells were not dead by this criterion (Figure 4A, 24 h, middle column). In fact, in most experiments they regrew more than in the absence of DIF-1, suggesting that under circumstances where DIF-1 is unable to induce death it might increase proliferation. All cells regrew less when HL5 rich medium was added at 40 h rather than at 24 h post-DIF-1 (Figure 4A, 40 h), showing that clonogenic cell death was not prevented but markedly delayed. In contrast, similar to wild-type cells DhkM^{del} mutant cells did not regrow after having been subjected to DIF-1 (Figure 4A, 24 h, right column). Thus, by regrowth tests the DhkM^{ins} but not the DhkM^{del} mutation impaired clonogenic cell death.

By staining tests at 40 h post-DIF-1, as expected (Cornillon *et al*., 1994) many HMX44A wild-type cells were vacuolated, and most of these showed FDA negativity/PI positivity (Figure 4B, left column). In contrast, most HMX44A.DhkM^{ins} and also DhkM^{del} mutant cells showed FDA positivity/PI negativity (Figure 4B, center and right columns). This indicated that at the moment of the FDA/PI tests both *ins* and *del* DIF-1–treated mutant cells still had intact plasma membranes; thus, they were not morphologically dead. Videos confirmed that at 40 h post-DIF-1, the majority of *del* cells were still alive in terms of morphological integrity and of intracellular movements (data not shown). Together, HMX44A.DhkM^{del} cells subjected to DIF-1 died clonogenically but not morphologically, dissociating these criteria of cell death. The *del* mutation thus prevented morphological but not clonogenic cell death, whereas the *ins* mutation prevented both. These and other results above led to mapping the steps inhibited by *ins* and *del* mutations and to propose a modified pathway scheme for ACD, as shown below (see Figure 6).

We also checked whether DhkM mutations affected cell death pathways other than ACD proper. The ACD-impairing DhkM mutations were probably not impairing the effects of starvation, because DhkM mutant cells subjected to only starvation showed the same phenotype as wild-type cells (data not shown). Necrotic cell death (NCD) occurs when cells mutated for atg1 are starved and exposed to DIF-1 (Kosta *et al*., 2004; Laporte *et al*., 2007; Giusti *et al*., 2009a). To test whether the DhkM mutations affected DIF-1–initiated pathways leading not only to ACD but also to NCD, we prepared HMX44A.atg1-3.DhkM^{ins} double mutants. When subjected to starvation and DIF-1, HMX44A.atg1-3.DhkM^{ins} were indistinguishable from HMX44A.atg1-3 cells in terms of morphology, kinetics, and DIF-1 dose–response curves (data not shown), showing that DhkM^{ins}, which prevented ACD, did not affect NCD.

The availability of DhkM mutations on the DH1 and JH10 backgrounds allowed us to test their impact on development. Compared with their wild-type counterparts, both DH1 and JH10 DhkM mutants showed delayed development. After ~40 h of development on agar, in mutants but not in wild type there were persistent slugs in parallel with apparently normal fruiting bodies (Figure 4C; data not shown). These results showed DhkM requirement for normal progression of development. We did not investigate in more detail other possible minor developmental abnormalities of DH1 and JH10 DhkM mutants. Developmental ab-

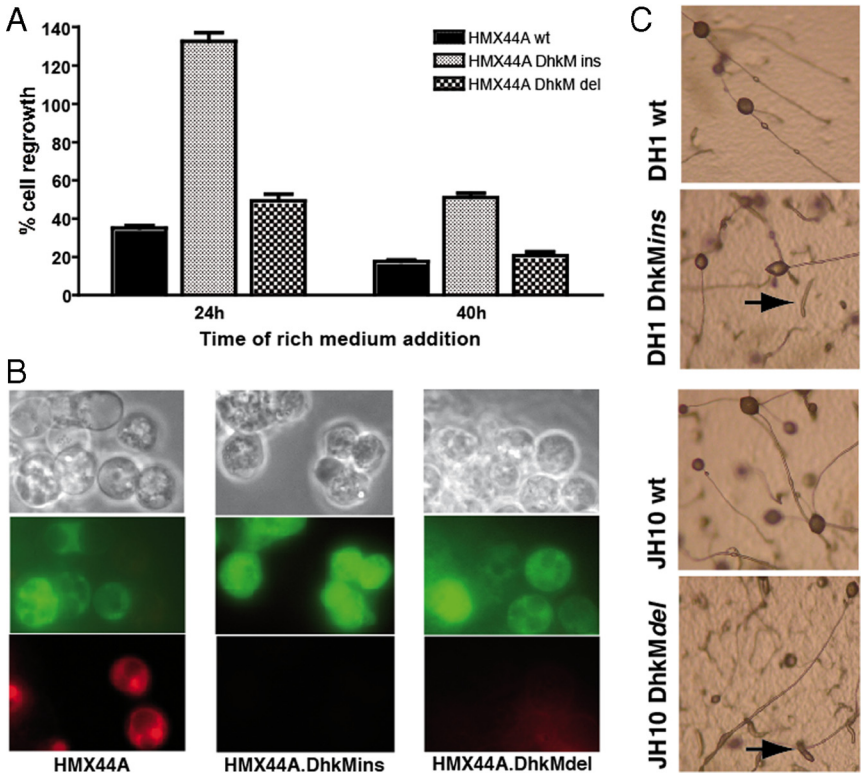

Figure 4. Effects of DhkM mutants on cell death and on development. (A and B) Delayed cell death in HMX44A DhkM mutant cells shown through two distinct tests. (A) Regrowth test. Wild-type or mutant cells were treated with DIF-1, and then HL5 rich medium was added at 24 or 48 h after DIF-1 within the same experiment. Surviving cells regrew in this medium, and their progeny were counted after another 48 or 72 h. Numbers of experimental cells were expressed as percentage of numbers of control cells without DIF-1; three separate Lab-Tek wells were used per group and error bars represent the SD. Especially *ins* mutant cells survived at 24 h post-DIF-1 much better than *del* or wild-type cells. This entire experiment was done twice with the same results. The *del* mutant cells showed in four of four independent regrowth tests much lower survival than *ins* cells. (B) Double staining with fluorescein diacetate (green) and propidium iodide (red) at 40 h post-DIF-1. More DhkM mutant cells are green and less are red than wild-type cells, in line with delayed cell death in mutant cells. (C) Development on agar for 40 h of wild-type or DhkM mutant cells on the DH1 or JH10 backgrounds. Fruiting bodies were present for both wild-type and mutant cells, whereas in mutant cells slugs persisted (arrows) even at 40 h after initiation of development, indicating delayed development in DhkM mutant cells.

normalities, sometimes with a similar "slugger" phenotype, were observed in mutants of other histidine kinase receptor genes in *Dictyostelium* (Schuster *et al*., 1996; Singleton *et al*., 1998; Zinda and Singleton, 1998; Wang *et al*., 1999; Thomason *et al*., 2006).

8-Bromo-cAMP Restored Vacuolization and Death in DhkM but Also iplA⁻ Mutant Cells

As shown in particular for DhkA (Wang *et al*., 1996), a histidine kinase receptor can phosphorylate and thus inactivate the phosphodiesterase regA. This would lead to an increase in intracellular cAMP concentration, thus activating protein kinase A (PKA), which in turn would phosphorylate a given set of molecules leading to given functions. A mutation of this histidine kinase receptor would prevent cAMP increase and downstream events. Addition of exogenous 8-bromo-cAMP (cell permeant and relatively insensitive to phosphodiesterases) would lead to an increase in intracellular cAMP even in these mutant cells and thus "suppress" the effects of the mutation by triggering PKA activation and downstream events.

In the absence of DIF-1, in agreement with previous results (Kay *et al*., 1988; Kay, 1989) addition of 8-bromo-cAMP to starved HMX44A cells led to differentiation into ovoid, cellulose-coated spore cells (data not shown). This was the case not only for wild-type cells but also for both DhkM^{ins} and DhkM^{del} mutant cells (data not shown), showing that these mutations did not prevent spore formation under these circumstances.

Events were quite different if DIF-1 was added (Kay *et al*., 1988; Kay, 1989). In the present model, addition of 20 mM 8-bromo-cAMP 19 h after addition of DIF-1 (or at the same time as DIF-1) led in wild-type cells to accelerated vacuolization (within 6–7 h rather than 20–24 h; data not shown), and, strikingly, in both *ins* and *del* DhkM mutant cells to cell rounding and marked vacuolization (Figure 5A; data not shown), also in an accelerated manner (Supplemental Video 3). This marked vacuolization induced by 8-bromo-cAMP in otherwise nonvacuolizing mutants did not occur if 8-bromo-cAMP was added at <5 mM, or in the absence of DIF-1 (data not shown). Also, the same 20 mM concentrations of sorbitol or of cAMP did not induce this vacuolization (Figure 5B), showing that vacuolization by exogenous 8-bromo-cAMP of normally nonvacuolizing DhkM mutant cells was not induced by variations in osmotic pressure or by extracellular cAMP. Not only vacuolization but also cell death was restored by 8-bromo-cAMP (Figure 5C). 8-Bromo-cAMP did not complement the mutations in the absence of initial starvation or DIF-1 (data not shown). Thus, the ACD pathway had to be brought to a certain stage(s) for 8-bromo-cAMP to push it further.

Restoration by 8-bromo-cAMP of vacuolization for both *ins* and *del* mutations suggested that both mutations led to comparable complementable cAMP depletion. However, 8-bromo-cAMP could restore vacuolization also in *iplA* mutants (Figure 5D). Also, when 8-bromo-cAMP was added, the ACD pathway proceeded in the usual sequence of events from the point of addition. For example, DhkM^{ins} mutant cells blocked as paddle cells evolved upon addition of 8-bromo-cAMP to round, then cellulose-encapsulated, then vacuolated cells (Supplemental Video 3; data not shown). This could occur at at least the two different locations in the pathway corresponding to the DhkM^{ins} and DhkM^{del} mutations that froze the pathway unless 8-bromo-cAMP was added. This seemed to exclude the possibility that 8-bromo-cAMP acted at only one point downstream in the pathway, by-passing most steps of the ACD cascade of events to lead to vacuolization. Rather, 8-bromo-cAMP could act at at least two points in this cascade, "just" downstream of the iplA/TalB/DhkM^{ins} mutants, and "just" downstream of the Dh-

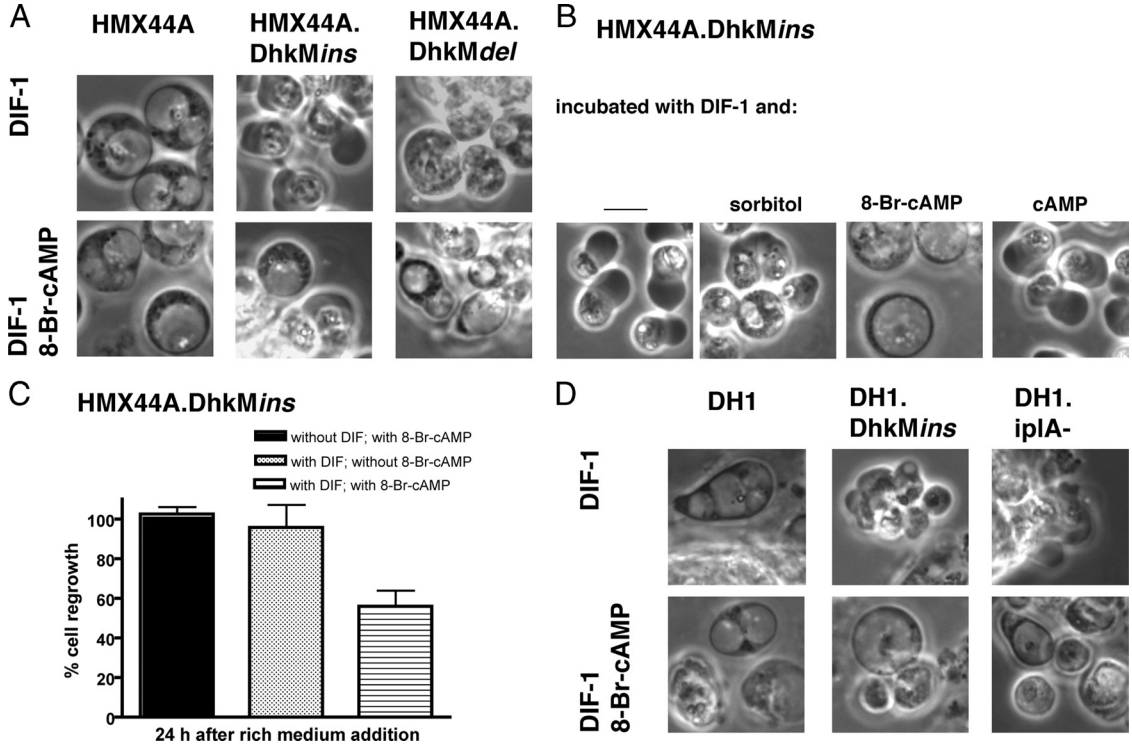

Figure 5. Restoration by 8-bromo-cAMP of vacuolization and death in DhkM mutant cells. (A) HMX44A wild-type or DhkM^{ins} or DhkM^{del} mutant cells were incubated with DIF-1, with or without addition of 8-bromo-cAMP at 16 h post-DIF-1. The addition of 8-bromo-cAMP restored vacuolization in DhkM mutant cell lines. (B) Sorbitol, 8-bromo-cAMP, or cAMP was added to starved HMX44A.DhkM^{ins} cells incubated for 16 h with DIF-1. Only 8-bromo-cAMP induced vacuolization in DhkM mutant cells. This was the case also if 8-bromo-cAMP was added 30 min before DIF-1 (data not shown). Also, the same results were obtained in the same experiment with *del* mutant cells. Pictures were taken 40 h post-DIF-1. (C) HMX44A.DhkM^{ins} cells were incubated with or without 8-bromo-cAMP and with or without DIF-1. The regrowth ability, tested by adding HL-5 medium 24 h post DIF-1, expressed as %=percentage of values without DIF-1 and 8-bromo-cAMP, was markedly less with DIF-1 in the presence of 8-bromo-cAMP. (D) Starved DH1 wild-type or DhkM^{ins} or iplA^{-} cells were incubated with DIF-1, in the presence or absence of 8-bromo-cAMP. Added 8-bromo-cAMP restored vacuolization in both DH1.DhkM^{ins} and DH1.iplA^{-} mutant cells.

kM^{del} mutants, respectively, leading to continuation of the cascade from each of these two points. This suggests that 8-bromo-cAMP acted as a substitute for DhkM, activating for instance PKA, which then phosphorylated distinct sets of proteins and had distinct effects at two distinct sites of the ACD pathway, allowing this pathway to proceed.

DISCUSSION

We reported previously on a series of mutants contributing to the molecular characterization of cell death pathways in *Dictyostelium* (Figure 6 and its legend). We report here on receptor histidine kinase DhkM mutants that showed the involvement of this receptor histidine kinase in ACD and that led to further downstream genetic definition of the ACD pathway. Depending on the nature of the DhkM mutation, ACD was blocked at distinct stages of the ACD pathway.

In eukaryotes, histidine protein kinase domains are often found in dimeric transmembrane receptors. These receptors sense the environment, including developmental signals, through their extracellular domains, and then transduce information to the interior of the cell (Hoch, 2000; Thomason and Kay, 2000; Wolanin *et al*., 2002; Goldberg *et al*., 2006). The intracellular part of these molecules can autophosphorylate by transferring a phosphate from ATP to a conserved histidine residue and then relay this phosphorylation to a conserved aspartate in a carboxy-terminal response regulator receiver domain, in the same "hybrid kinase" molecule. Phosphates are then further transferred to intermediate histidine phosphotransfer proteins (such as RdeA in *Dictyostelium*) and then to downstream response regulators (such as the RegA phosphodiesterase in *Dictyostelium*). In *Dictyostelium*, there are 14 known histidine kinases, of which five, including DhkM, encode putative transmembrane domains. Although other genes among the known histidine kinase genes in *Dictyostelium* have been inactivated, such as DhkA (Wang *et al*., 1999), DhkB (Zinda and Singleton, 1998), DhkC (Singleton *et al*., 1998), DhkK (Thomason *et al*., 2006), and DokA (Schuster *et al*., 1996), we are not aware of previous reports on inactivation of DhkM. According to published expression profiles, DhkM mRNA expression increased after 5 h of development (VanDriessche *et al*., 2002; Iranfar *et al*., 2003), whereas in the present work it did not significantly vary throughout differentiation from vegetative to "stalk" cells in vitro.

Histidine kinases are found in abundance in most kingdoms of life, but not in animals. However, their kinase activity may be ensured at functionally homologous steps by other kinases. For example, receptor histidine kinases function analogously to growth factor receptors with tyrosine kinase activity in animal cells. There are no known examples of organisms that have both receptor tyrosine kinases and receptor histidine kinases, suggesting that these receptors

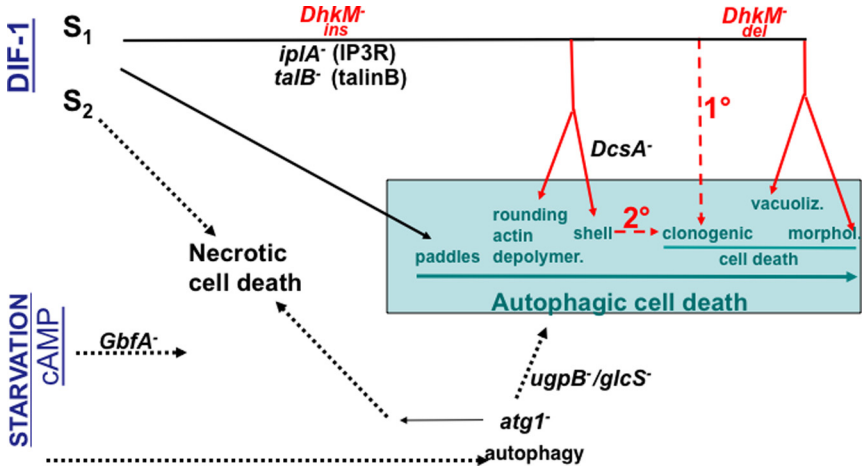

Figure 6. Provisional schematic representation of pathways controlling cell death in *Dictyostelium*. The ACD phenotype is light blue boxed, pathways controlling this phenotype and the NCD phenotype are shown as black arrows, and inducers are in blue. In red, mutations and pathways whose positions have been clarified in this report. Both ACD and NCD required a first signal provided by starvation and cAMP (bottom), which was impaired by GbfA (Giusti *et al*., 2009b) or ugpB/glcS (Tresse *et al*., 2008) mutations. Mutations of atg1 suppressed ACD (unpublished data) and led to the induction of NCD (Kosta *et al*., 2004; Laporte *et al*., 2007; Giusti *et al*., 2009a). A second signal provided by exogenous DIF-1 led to either ACD or to NCD when atg1 was mutated. DIF-1 was recognized by distinct structures, designated here as S_1 and S_2, at the onset of either ACD or NCD (Luciani *et al*., 2009). More specifically, the control of ACD is detailed in the top of the figure. It included induction of paddle cells, spared by the iplA (Lam *et al*., 2008), talB (Giusti *et al*., 2009b), and DhlM^{ins} mutations, which impaired the rest of ACD. DhkM mutations affected the ACD control pathway at two distinct steps. At a location in the ACD pathway not easily separable so far from those of iplA and talinB, the DhkM^{ins} mutation inhibited the paddle-to-round transition normally leading to rounding and cellulose synthesis (itself under the control of the DcsA cellulose synthase; Blanton *et al*., 2000; Levraud *et al*., 2003). More downstream, the round-to-vacuolar transition normally led to vacuolization and cell death. The DhkM^{del} mutation inhibited vacuolization and morphological (defined by cell membrane rupture) but not clonogenic (defined by inability to regrow) cell death. Dotted red lines show primary or secondary pathways to clonogenic cell death. To facilitate graphic representation, the temporal sequence of ACD subcellular events and its control molecular sequence are shown here as colinear, but they need not be so. More specifically, the molecules involved in the *ins* and *del* mutations may be in spatial proximity.

may fulfill equivalent roles (Wolanin *et al*., 2002, but see Fang *et al*., 2007).

DhkM mutants obtained by random then targeted mutagenesis unexpectedly affected not one but either of two transitions in the ACD pathway (Figure 6). The *del* mutation presumably led to at least major functional impairment of the DhkM protein and to impairment of vacuolization and of morphological cell death. Thus, importantly, the *del* mutation may reveal a normal function of DhkM, leading from rounding to vacuolization and morphological cell death. The *del* mutation dissociated the latter, which it prevented, from actin depolymerization, cellulose synthesis and clonogenic cell death, which it apparently did not affect (Figure 6). Thus, the control of vacuolization and morphological cell death on the one hand and of clonogenic cell death on the other hand seemed distinct in the ACD pathway in *Dictyostelium*. Clonogenic cell death might be a primary consequence of DIF-1 triggering (1° in Figure 6), through for example a direct alteration of the mitotic machinery, or a secondary consequence of it (2° in Figure 6) through, for example, actin depolymerization, cellulose shell formation, or both. As a note of caution, cell death occurring in *del* mutant and in wild-type ACD may not necessarily follow the same molecular mechanism. This may be revealed by further mutations. Together, the DhlM^{del} mutation genetically dissociated late events in the ACD pathway, downstream of rounding and cellulose synthesis.

Studying effects of the *del* mutation also led to observations of *Dictyostelium* cells wrapping the cellulose pegs surrounding DIF-1–induced mutant cells. This probably involved on *Dictyostelium* cells cellulose-binding domains (Wang *et al*., 2001) or molecules binding to cellulose-associated material. Similar-looking cell-in-cell appearances have been reported in particular in mammalian cells and are usually ascribed to cells wandering into other cells (emperipolesis) that they enter by engulfment or invasion (Overholtzer and Brugge, 2008). This explanation cannot apply to the present situation, because the "internal" cells are stuck to the substrate. Other apparently similar observations in *Dictyostelium* (Waddell, 1982; Lewis and O'Day, 1986; Tatischeff *et al*., 2001; Nizak *et al*., 2007) are probably unrelated to the present ones. Together, the cell-in-cell appearances seen here were due to wrapping not engulfment.

The *ins* mutation, which crippled but presumably did not eliminate the DhkM protein, impaired the ACD pathway upstream of the step inhibited by the *del* mutation. More specifically, the *ins* mutation inhibited the paddle-to-round transition and thus prevented actin depolymerization, cellulose synthesis, and also both vacuolization and cell death. In retrospect, our selection and screening strategy logically yielded not a *del* but an *ins* mutant, which was unable to die (as selected for) and to vacuolize (as screened for). Of note, DhkM was not as such required for the paddle-to-round transition, because this transition occurred normally in the *del* mutant in the absence of functional DhkM. The *ins* mutation must have endowed the mutated DhkM with a novel property, namely, inhibition of the paddle-to-round transition, perhaps through a dominant-negative effect of altered DhkM. Thus, the *ins* mutation may reveal not a normal function of DhkM but a property of only the crippled DhkM molecule. The DhkM^{ins} mutation dissociated paddle cell formation from further events, similarly to the iplA and TalinB mutations. However, iplA and DhkM^{ins} mutants did not have exactly the same phenotype. DhkM^{ins} mutants showed more regrowth than iplA mutants (compare Lam *et al*., 2008 and the present data). Also, the phenotypic expression of DhkM^{ins} was more marked in HMX44A than in DH1 cells (this study), whereas the reverse was true for iplA or TalinB mutants (Lam *et al*., 2008; Giusti *et al*., 2009b). Together, DhkM^{ins} and iplA^{-} mutants impaired the same region of the ACD pathway, upstream of rounding and cellulose synthesis.

DhkM is a receptor kinase. We do not know what the ligand(s) of the DhkM might be, although it is tempting to speculate that it may correspond to already known molecules involved in *Dictyostelium* differentiation. In *Dictyostelium*, ligands, stimuli, or a combination already identified or considered for receptor histidine kinases are SDF-2 (DhkA),

discadenine (DhkB), ammonia (DhkC), and osmolarity (DokA) (Schuster *et al*., 1996; Singleton *et al*., 1998; Zinda and Singleton, 1998; Wang *et al*., 1999). It is believed that several of these histidine kinases control cAMP levels by signaling to the response regulator phosphodiesterase RegA, probably coordinated with cAMP-controlling G protein-dependent pathways (Wolanin *et al*., 2002). Phosphorylation of RegA strongly stimulates its phosphodiesterase activity (Thomason *et al*., 1999). Interestingly, DhkA$^-$ mutant cells show markedly reduced levels of cAMP (Tekinay *et al*., 2003). Trying to complement the DhkM mutations with exogenous 8-bromo-cAMP (Wang *et al*., 1996) indeed led in the present model to vacuolization and cell death in not only DhkM mutant cells but also in iplA mutant cells. These and further results suggested that 8-bromo-cAMP could lead at two different points in the ACD pathway, marked by the *ins* and *del* DhkM mutations, to activation of PKA and subsequent phosphorylation of distinct sets of proteins, with distinct functional consequences along the ACD pathway. An alternative and more parsimonious explanation is that 8-bromo-cAMP somehow just greatly accelerates the ACD pathway, leading to early vacuolization in normally vacuolization-delayed mutants.

Interestingly, in developmentally competent strains, although DhkM mutations prevented cell death in monolayers, they did not prevent stalk cell differentiation upon development. This is somewhat reminiscent of mutations preventing DIF-1 synthesis and therefore impairing cell death in monolayers but not affecting development. Such apparent discrepancies between in vivo and in vitro results could be due to differences in cell–cell contacts, presence of an extracellular matrix, or effects of extracellular signals.

DIF-1 might be considered a prototypic second signal for autophagic cell death. The DIF-1–triggered second signal in *Dictyostelium* ACD may be functionally homologous to a putative second signal for ACD in higher eukaryotes, as hypothesized previously (Giusti *et al*., 2009b). Its analysis may thus provide hints as to corresponding molecular mechanisms in higher eukaryotes. Investigations downstream of DhkM (for example by looking for DhkM-interacting molecules, or for molecules phosphorylated through the kinase function of DhkM, or for further mutants with a phenotype similar to that of DhkM mutants) may provide more information on the molecular mechanisms of vacuolization and cell death. Although DhkM itself is not phylogenetically conserved, it may lead to downstream molecules involved in these traits and phylogenetically conserved.

From another point of view, apparently several extracellular ligands (such as cAMP, DIF-1 itself, and the putative ligand of DhkM if distinct) play a role in series in the induction and course of *Dictyostelium* cell death. It follows that cell death in this case is controlled by the environment through repeated extracellular signaling and thus is not cell autonomous. Also, at least some effects of DIF-1 are transcription factor dependent (Thompson *et al*., 2004; Huang *et al*., 2006; Zhukovskaya *et al*., 2006), and it would be of great interest to integrate this set of data and the sequence of events described here.

ACKNOWLEDGMENTS

We thank L. Aubry, G. Klein, and J. Ewbank for helpful discussions and reading the manuscript. We thank Institut National de la Santé et de la Recherche Médicale and Centre National de la Recherche Scientifique for institutional support, and for grants we thank Agence Nationale pour la Recherche (DictyDeath ANR-05-BLAN-0333-01), the European Community (FP6 STREP TransDeath LSHG-CT-2004-511983), and Association pour la Recherche sur le Cancer.

REFERENCES

Berry, D. L., and Baehrecke, E. H. (2008). Autophagy functions in programmed cell death. Autophagy *4*, 359–360.

Blanton, R. L., Fuller, D., Iranfar, N., Grimson, M. J., and Loomis, W. F. (2000). The cellulose synthase gene of *Dictyostelium*. Proc. Natl. Acad. Sci. USA *97*, 2391–2396.

Cornillon, S., Foa, C., Davoust, J., Buonavista, N., Gross, J. D., and Golstein, P. (1994). Programmed cell death in *Dictyostelium*. J. Cell Sci. *107*, 2691–2704.

de Chastellier, C., and Ryter, A. (1977). Changes of the cell surface and of the digestive apparatus of *Dictyostelium discoïdeum* during the starvation period triggering aggregation. J. Cell Biol. *75*, 218–236.

Dove, S. K., Dong, K., Kobayashi, T., Williams, F. K., and Michell, R. H. (2009). Phosphatidylinositol 3,5-bisphosphate and Fab1p/PIKfyve under PPIn endolysosome function. Biochem. J. *419*, 1–13.

Eisenberg-Lerner, A., Bialik, S., Simon, H. U., and Kimchi, A. (2009). Life and death partners: apoptosis, autophagy and the cross-talk between them. Cell Death Diff. *16*, 966–975.

Fang, J., Brzostowski, J. A., Ou, S., Isik, N., Nair, V., and Jin, T. (2007). A vesicle surface tyrosine kinase regulates phagosome maturation. J. Cell Biol. *178*, 411–423.

Giusti, C., Luciani, M. F., Klein, G., Aubry, L., Tresse, E., Kosta, A., and Golstein, P. (2009a). Necrotic cell death: from reversible mitochondrial uncoupling to irreversible lysosomal permeabilization. Exp. Cell Res. *315*, 26–38.

Giusti, C., Tresse, E., Luciani, M.-F., and Golstein, P. (2009b). Autophagic cell death: analysis in *Dictyostelium*. Biochim. Biophys. Acta Mol. Cell Biol. *1793*, 1422–1431.

Goldberg, J. M., Manning, G., Liu, A., Fey, P., Pilcher, K. E., Xu, Y., and Smith, J. L. (2006). The *Dictyostelium* kinome–analysis of the protein kinases from a simple model organism. PLoS Genet. *2*, e38.

Hoch, J. A. (2000). Two-component and phosphorelay signal transduction. Curr. Opin. Microbiol. *3*, 165–170.

Huang, E., Blagg, S. L., Keller, T., Katoh, M., Shaulsky, G., and Thompson, C. R. (2006). bZIP transcription factor interactions regulate DIF responses in *Dictyostelium*. Development *133*, 449–458.

Iranfar, N., Fuller, D., and Loomis, W. F. (2003). Genome-wide expression analyses of gene regulation during early development of *Dictyostelium discoideum*. Eukaryot. Cell *2*, 664–670.

Kay, R. R. (1987). Cell differentiation in monolayers and the investigation of slime mold morphogens. Methods Cell Biol. *28*, 433–448.

Kay, R. R. (1989). Evidence that elevated intracellular cyclic AMP triggers spore maturation in *Dictyostelium*. Development *105*, 753–759.

Kay, R. R., Berks, M., Traynor, D., Taylor, G. W., Masento, M. S., and Morris, H. R. (1988). Signals controlling cell differentiation and pattern formation in *Dictyostelium*. Dev. Genet. *9*, 579–587.

Keim, M., Williams, R. S., and Harwood, A. J. (2004). An inverse PCR technique to rapidly isolate the flanking DNA of *Dictyostelium* insertion mutants. Mol. Biotechnol. *26*, 221–224.

Kosta, A., Roisin-Bouffay, C., Luciani, M. F., Otto, G. P., Kessin, R. H., and Golstein, P. (2004). Autophagy gene disruption reveals a non-vacuolar cell death pathway in *Dictyostelium*. J. Biol. Chem. *279*, 48404–48409.

Kuspa, A., and Loomis, W. F. (1992). Tagging developmental genes in *Dictyostelium* by restriction enzyme-mediated integration of plasmid DNA. Proc. Natl. Acad. Sci. USA *89*, 8803–8807.

Lam, D., Kosta, A., Luciani, M. F., and Golstein, P. (2008). The IP3 receptor is required to signal autophagic cell death. Mol. Biol. Cell *19*, 691–700.

Laporte, C., Kosta, A., Klein, G., Aubry, L., Lam, D., Tresse, E., Luciani, M. F., and Golstein, P. (2007). A necrotic cell death model in a protist. Cell Death Diff. *14*, 266–274.

Levraud, J.-P., Adam, M., Luciani, M.-F., De Chastellier, C., Blanton, R. L., and Golstein, P. (2003). *Dictyostelium* cell death: early emergence and demise of highly polarized paddle cells. J. Cell Biol. *160*, 1105–1114.

Lewis, K. E., and O'Day, D. H. (1986). Phagocytic specificity during sexual development in *Dictyostelium discoideum*. Can. J. Microbiol. *32*, 79–82.

Luciani, M. F., Kubohara, Y., Kikuchi, H., Oshima, Y., and Golstein, P. (2009). Autophagic or necrotic cell death triggered by distinct motifs of the differentiation factor DIF-1. Cell Death Diff. *16*, 564–570.

Morris, H. R., Taylor, G. W., Masento, M. S., Jermyn, K. A., and Kay, R. R. (1987). Chemical structure of the morphogen differentiation inducing factor from *Dictyostelium discoideum*. Nature *328*, 811–814.

Nizak, C., Fitzhenry, R. J., and Kessin, R. H. (2007). Exploitation of other social amoebae by *Dictyostelium caveatum*. PloS One *2*, e212.

Overholtzer, M., and Brugge, J. S. (2008). The cell biology of cell-in-cell structures. Nat. Rev. *9*, 796–809.

Raper, K. B. (1935). *Dictyostelium discoideum*, a new species of slime mold from decaying forest leaves. J. Agric. Res. *50*, 135–147.

Schuster, S. C., Noegel, A. A., Oehme, F., Gerisch, G., and Simon, M. I. (1996). The hybrid histidine kinase DokA is part of the osmotic response system of *Dictyostelium*. EMBO J. *15*, 3880–3889.

Singleton, C. K., Zinda, M. J., Mykytka, B., and Yang, P. (1998). The histidine kinase dhkC regulates the choice between migrating slugs and terminal differentiation in *Dictyostelium discoideum*. Dev. Biol. *203*, 345–357.

Tatischeff, I., Petit, P. X., Grodet, A., Tissier, J. P., Duband-Goulet, I., and Ameisen, J. C. (2001). Inhibition of multicellular development switches cell death of *Dictyostelium discoideum* towards mammalian-like unicellular apoptosis. Eur. J. Cell Biol. *80*, 428–441.

Tekinay, T., Ennis, H. L., Wu, M. Y., Nelson, M., Kessin, R. H., and Ratner, D. I. (2003). Genetic interactions of the E3 ubiquitin ligase component FbxA with cyclic AMP metabolism and a histidine kinase signaling pathway during *Dictyostelium discoideum* development. Eukaryot. Cell *2*, 618–626.

Thomason, P., and Kay, R. (2000). Eukaryotic signal transduction via histidine-aspartate phosphorelay. J. Cell Sci. *113*, 3141–3150.

Thomason, P. A., Sawai, S., Stock, J. B., and Cox, E. C. (2006). The histidine kinase homologue DhkK/Sombrero controls morphogenesis in *Dictyostelium*. Dev. Biol. *292*, 358–370.

Thomason, P. A., Traynor, D., Stock, J. B., and Kay, R. R. (1999). The RdeA-RegA system, a eukaryotic phospho-relay controlling cAMP breakdown. J. Biol. Chem. *274*, 27379–27384.

Thompson, C. R., Fu, Q., Buhay, C., Kay, R. R., and Shaulsky, G. (2004). A bZIP/bRLZ transcription factor required for DIF signaling in *Dictyostelium*. Development *131*, 513–523.

Tresse, E., Kosta, A., Giusti, C., Luciani, M. F., and Golstein, P. (2008). A UDP-glucose derivative is required for vacuolar autophagic cell death. Autophagy *4*, 680–691.

VanDriessche, N., *et al*. (2002). A transcriptional profile of multicellular development in *Dictyostelium discoideum*. Development *129*, 1543–1552.

Waddell, D. R. (1982). A predatory slime mould. Nature *298*, 464–466.

Wang, N., Shaulsky, G., Escalante, R., and Loomis, W. F. (1996). A two-component histidine kinase gene that functions in *Dictyostelium* development. EMBO J. *15*, 3890–3898.

Wang, N., Soderbom, F., Anjard, C., Shaulsky, G., and Loomis, W. F. (1999). SDF-2 induction of terminal differentiation in *Dictyostelium discoideum* is mediated by the membrane-spanning sensor kinase DhkA. Mol. Cell Biol. *19*, 4750–4756.

Wang, Y. Z., Slade, M. B., Gooley, A. A., Atwell, B. J., and Williams, K. L. (2001). Cellulose-binding modules from extracellular matrix proteins of *Dictyostelium discoideum* stalk and sheath. Eur. J. Biochem. *268*, 4334–4345.

Wolanin, P. M., Thomason, P. A., and Stock, J. B. (2002). Histidine protein kinases: key signal transducers outside the animal kingdom. Genome Biol. *3*, REVIEWS3013.

Zhukovskaya, N. V., Fukuzawa, M., Yamada, Y., Araki, T., and Williams, J. G. (2006). The *Dictyostelium* bZIP transcription factor DimB regulates prestalk-specific gene expression. Development *133*, 439–448.

Zinda, M. J., and Singleton, C. K. (1998). The hybrid histidine kinase dhkB regulates spore germination in *Dictyostelium discoideum*. Dev. Biol. *196*, 171–183.